Postgrowth annealing of defects in ZnO studied by positron annihilation, x-ray diffraction, Rutherford backscattering, cathodoluminescence, and Hall measurements

Z. Q. Chen,[a] S. Yamamoto, M. Maekawa, and A. Kawasuso
Japan Atomic Energy Research Institute, 1233 Watanuki, Takasaki, Gunma 370-1292, Japan

X. L. Yuan and T. Sekiguchi
Nanomaterials Laboratory, National Institute for Materials Science, 1-2-1 Sengen, Tsukuba, Ibaraki 305-0047, Japan

(Received 20 March 2003; accepted 23 July 2003)

Defects in hydrothermal grown ZnO single crystals are studied as a function of annealing temperature using positron annihilation, x-ray diffraction, Rutherford backscattering, Hall, and cathodoluminescence measurements. Positron lifetime measurements reveal the existence of Zn vacancy related defects in the as-grown state. The positron lifetime decreases upon annealing above 600 °C, which implies the disappearance of Zn vacancy related defects, and then remains constant up to 900 °C. The Rutherford backscattering and x-ray rocking curve measurements show the improvement of crystal quality due to annealing above 600 °C. Although the crystal quality monitored by x-ray diffraction measurements is further improved after annealing at above 1000 °C, the positron lifetime starts to increase. This is due to either the formation of Zn vacancy related defects, or the change of the Zn vacancy charge state occupancy as a result of the Fermi level movement. The electron concentration increases continuously with increasing annealing temperature up to 1200 °C, indicating the formation of excess donors, such as oxygen vacancies or zinc interstitials. The cathodoluminescence measurements reveal that the ultraviolet emission is greatly enhanced in the same temperature range. The experimental results show that the ZnO crystal quality, electrical and optical characteristics are improved by postgrowth annealing from 600 to 1200 °C. The disappearance of Zn vacancy related defects contributes to the initial stage of improved crystal quality. © *2003 American Institute of Physics.* [DOI: 10.1063/1.1609050]

I. INTRODUCTION

Over the years the polycrystalline zinc oxide (ZnO) has been found to have wide applications including piezoelectric transducers, varistors, phosphors, and transparent conducting films.[1] As a wide-gap (3.37 eV at room temperature) semiconductor, it is now attracting more attention. Recent success in producing large-area single crystals[2] revealed that ZnO has potential optoelectronic applications in blue and UV light emitting devices due to the wide band gap and large exciton binding energy (60 meV).[3,4] The close match in the lattice constant with GaN also allows it to be a good substrate material for GaN based devices. ZnO is well poised for space applications, since it is fairly resistant to radiation damage compared with other semiconductors.[5]

The key factor to assure the high performance of semiconductor devices is high quality crystals. However, in semiconductors various defects often exist which affect the electrical and optical properties. In ZnO, for example, undoped materials mostly exhibit *n*-type conductivity. This is supposed to be due to the existence of native point defects, such as oxygen vacancies and Zn interstitials. Like many other wide-gap semiconductors, there exists a so-called doping asymmetry,[6] that is, it is easy to get *n*-type ZnO, but rather difficult to produce *p*-type ZnO. One of the possible mechanisms leading to the doping difficulty is the self-compensation by native defects, which has prevented the production of ZnO based devices such as UV-emitting diodes. Some defects also reduce the device lifetime and decrease the light emission efficiency. For example, dislocations act as nonradiative recombination centers and suppress the UV emission. Control of the defects so as to improve the quality of the materials has been proven to be very important. Study of the microstructure of these defects in ZnO is necessary to provide the guidance to control these defects.

The defects in ZnO are characterized by a variety of experimental methods, such as electron paramagnetic resonance, photoluminescence, cathodoluminescence (CL), x-ray diffraction (XRD), and deep level transient spectroscopy. Positron annihilation spectroscopy (PAS) has emerged as a powerful tool to investigate vacancy defects in semiconductors.[7] Positrons are trapped preferentially by vacancy defects. Annihilation characteristics of positrons are different in the perfect bulk state and vacancy trapped state. That is, positron lifetime at vacancy defect sites is longer, and the Doppler broadening of the annihilation radiation is narrower, as compared with those for bulk state. Up to now there are a few works on the study of defects in ZnO using PAS.[8–14] However, most of those studies were conducted on polycrystal ZnO, and hence, there are many fundamental

[a]Electronic mail: chenzq@taka.jaeri.go.jp

questions that still need to be solved, such as the scattering of the positron bulk lifetime ranging from 158 to 210 ps.[9–14] Although the reason is not yet fully understood, it seems that native vacancy defects have an important role in positron annihilation.

In this article, we studied the effect of heat treatment on the native defects in ZnO single crystals by PAS. Also XRD rocking curve, Rutherford backscattering (RBS), CL, and Hall measurements were performed to get a comprehensive understanding of the defect characteristics.

II. EXPERIMENT

Samples used in this study were hydrothermal-grown ZnO single crystals purchased from the Scientific Production Company (SPC). All the samples were undoped. The resistivity (ρ) is approximately 1.7×10^4 Ω cm. For comparison, undoped *n*-type ZnO single crystals purchased from Eagle Picher (EP)($\rho=0.5-1.5$ Ω cm) were used, which is grown by the seeded chemical vapor transport method. The SPC–ZnO samples were annealed isochronally in nitrogen atmosphere with temperature ranging from 100 to 1200 °C and annealing duration of 2 h.

The positron source was prepared by depositing ^{22}NaCl onto a Ti thin film with a thickness of 3 μm. Positron lifetime measurements were performed using a conventional fast-fast coincidence lifetime spectrometer with a time resolution of 210 ps in full width at half maximum (FWHM). No less than 10^6 total counts were accumulated in each measurement. The lifetime spectra were analyzed by a computer program called PATFIT.[15] The source component was determined to be 640 ps with an intensity of 2% using semi-insulating GaAs which has a density close to ZnO. To check the crystallographic quality of ZnO single crystals, RBS measurements were carried out using 2.0 MeV He^+ ions. The backscattered particles were detected at a scattering angle of 165°. At first we measured the backscattered spectra with He^+ ions incident at random direction. Then the He^+ ions were hit along the [0001] axis, and an aligned spectrum was recorded. The minimum yield $\chi_{\min}$, defined as the ratio of the aligned yield to the random yield for the same ion energy, was used to indicate the crystalline quality.[16,17] XRD rocking curve measurements were performed using a high-resolution diffractometer (X'Pert-MRD, Philips) and a Ge (2 2 0) asymmetric four-crystal monochromator for the incident beam to select the Cu K_α radiation. The Hall measurement was performed using the van der Pauw method[18] with gold (Au) ohmic electrodes. The samples were etched in HCl before fabricating the Au contact. The measurement was performed at room temperature. CL measurements were also performed at room temperature using a scanning electron microscope attached with a beam blanking system.[19] The electron beam energy was 5 keV.

III. RESULTS AND DISCUSSION

A. Structural characterizations

Positron lifetime measurements were first conducted to study the microstructure of ZnO. For all the samples, two component analysis of the positron lifetime spectra was rather difficult, only one lifetime component could be resolved after subtracting the source and background components. Positron lifetime obtained from the as-grown EP–ZnO is 171 ± 1 ps, while that from the as-grown SPC–ZnO is 189 ± 1 ps. This suggests that positrons are trapped by vacancy defects in the SPC–ZnO sample. Appearance of only one lifetime component is explained in several ways: the defect lifetime is close to the bulk value, the concentration of defects is rather low, or there are many positron trapping states with lifetime closely spaced to each other.

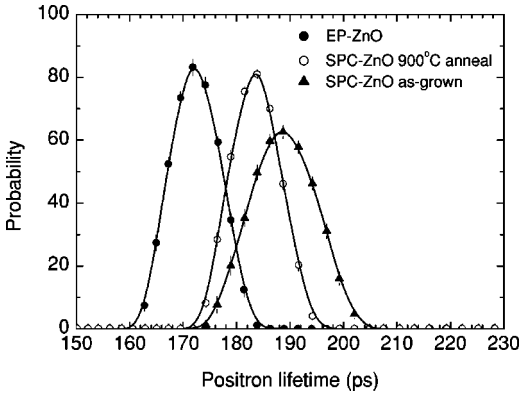

FIG. 1. Continuous positron lifetime distributions for the as-grown EP–ZnO, as-grown SPC–ZnO, and SPC–ZnO annealed at 900 °C in nitrogen ambient by CONTIN analysis.

To clarify these possibilities, we also used the Laplace inversion technique to analyze the positron lifetime spectra. Continuous positron lifetime distributions were obtained by the CONTIN program.[20] Figure 1 shows the positron lifetime distribution results obtained from the as-grown EP–ZnO, SPC–ZnO, and 900 °C annealed SPC–ZnO. As expected from the PATFIT analysis using the exponential function, only one peak was seen in each sample. The peak positions are in good agreement with the positron average lifetime obtained by PATFIT analysis, however, the peak widths are different depending on the samples. The FWHM of the distribution for the EP–ZnO is 9.5 ps. On the contrary, for the as-grown SPC–ZnO it is apparently wider, i.e., 12.6 ps. The narrow positron lifetime distribution for EP–ZnO indicates that positrons might annihilate from the delocalized bulk state. This lifetime is, however, a little higher than that reported previously for single crystalline ZnO, i.e., 158–169 ps.[12–14] Thus our EP–ZnO is likely to contain some positron traps with rather low concentration, or having a positron lifetime very close to that of the bulk, so the lifetime distribution is very narrow. The wider lifetime distribution for the as-grown SPC–ZnO therefore clearly indicates that positrons annihilate from both free and vacancy-trap states. Since the positron lifetimes of these states are close to each other, they are not separated.

The annealing experiment gives further evidence that positrons are trapped by vacancy defects in the as-grown SPC–ZnO. Figure 2 shows the annealing behavior of positron lifetime. It is found that after annealing at 600 °C the positron lifetime decreases from 189 to 181 ps and remains constant up to 900 °C. The width of positron lifetime distribution also decreases after annealing above 600 °C suggest-

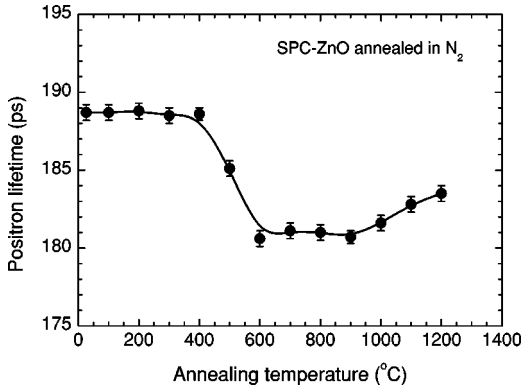

FIG. 2. Positron lifetime as a function of annealing temperature obtained for the SPC–ZnO. Annealing was conducted in a nitrogen ambient for 2 h.

ing the disappearance of vacancy defects. As seen from Fig. 1, the width of lifetime distribution after 900 °C annealing is nearly the same as that of the as-grown EP–ZnO. However, the positron lifetime after annealing is still 10 ps higher than that of EP–ZnO. It is hypothesized that in the 900 °C annealed SPC–ZnO, positrons have some kind of spatially averaged lifetime, which is correlated with the quality of the sample. In other words, positrons annihilate at some other sites other than the perfect lattice, such as impurities, small angle grain boundaries or some other unknown imperfections, which are distributed homogeneously inside the sample. Our supposition may explain why some papers report different positron bulk lifetimes in different ZnO samples. Therefore, even if there are vacancy defects in the as-grown SPC–ZnO, it is very difficult to separate the defect lifetime from the other lifetime components. This may be the reason for the single lifetime in the as-grown SPC–ZnO.

In ZnO, both Zn vacancy (V_{Zn}) and O vacancy (V_O) exist as native vacancies.[21] From the recent theoretical studies, V_{Zn} works as an acceptor and, hence, charges as negative when the Fermi level is higher than the acceptor level. Whereas V_O acts as a donor and only neutral or positive charge states are available.[21–23] Many experimental studies showed the existence of positive charge state associated with V_O.[24,25] Therefore, V_O may be a weaker positron trapping center than V_{Zn}.

We also examined the model of positron screening in semiconductors and insulators proposed by Puska *et al.*[26] to calculate the positron states in ZnO. In the calculation, the atomic superposition method[27] is used to get the electron density. The semiconductor model is used to calculate the enhancement of the electron density at the positron sites.[26] We constructed the supercell of ZnO which contains 128 atoms (64 zinc and 64 oxygen). Lattice relaxation around the vacancy is not taken into account in the calculation. The result shows that the localization of positron wave function at V_O is rather weak. The positron binding energy to V_O is only 0.04 eV, which is much lower than that of V_{Zn} (0.39 eV). The calculated positron bulk lifetime is about 158 ps, which is close to the experimental value reported previously.[12–14] The positron lifetime at V_O is about 160 ps, only 2 ps higher than the bulk value, while for V_{Zn}, the positron lifetime increases to 187 ps. Thus, V_O is essentially invisible in PAS measurement, and only Zn vacancies may be observable. This is a common phenomenon in metal oxides as predicted by Puska *et al.*[26] The higher positron lifetime in the as-grown SPC–ZnO is thus probably due to V_{Zn} related defects.

The disappearance of V_{Zn} related defects due to annealing may be interpreted in terms of recombination with Zn interstitials (I_{Zn}). It is known that in ZnO the oxygen vapor pressure is much higher than that of Zn. At elevated temperature, oxygen may evaporate first

$$\mathrm{ZnO} \rightarrow \mathrm{Zn_{Zn}} + \mathrm{V_O} + \tfrac{1}{2}\mathrm{O_2}\uparrow. \quad (1)$$

The evaporation of oxygen results in a stoichiometric excess of Zn. According to the theoretical calculation, V_O and I_{Zn} have relatively lower formation energies than the other defects,[23] especially in Zn rich condition. Therefore, it is easy to form I_{Zn} due to the reaction (1). At elevated temperatures, I_{Zn} becomes mobile to recombine with V_{Zn}. Ogata *et al.*[28] observed that in the molecular beam epitaxy grown ZnO layers, after annealing above 500 °C in nitrogen atmosphere, the electron carrier density increased. They ascribed this increase to the formation of I_{Zn} and V_O due to the evaporation of oxygen. Several other articles also reported that high temperature treatment of ZnO produced large amount of V_O and I_{Zn}.[29–31] It is also possible that the V_{Zn} and I_{Zn} coexist in the as-grown SPC–ZnO, and with increasing annealing temperature they mutually recombine. Another possibility explaining the disappearance of Zn vacancies may be the filling of vacant sites by impurity atoms. For example, the alkali metal impurities, which commonly exist in the hydrothermal grown ZnO crystals, may occupy Zn atom sites.

The change of positron lifetime may be also caused by the defect reaction with hydrogen. The hydrothermal grown crystal may contain a certain amount of hydrogen.[32] Such hydrogen may be combined with some defects in as-grown state. If such hydrogen is released from the defects after annealing at around 500–600 °C, the positron lifetime may be changed at this temperature. However, the CL experiments[33,34] suggest that the hydrogen is released from the defect which result in visible emission over 700 °C. Moreover, the release of hydrogen from vacancy type defects may result in the increase of positron lifetime, which is contrary to our result. Thus, it is rather difficult to attribute a decrease in the positron lifetime to the release of hydrogen from the defects.

As the annealing temperature increases higher than 1000 °C, the positron lifetime slightly increases. This increment of positron lifetime suggests possibly the formation of vacancy defects by heat treatment. It is probably due to the evaporation of Zn atom and subsequent introduction of Zn vacancies. There is also another possible reason for the increase of positron lifetime. As stated earlier, after annealing the electron concentration in ZnO will increase.[28] This is also confirmed by our Hall measurement, which will be discussed in the next section. Due to the increase of electron concentration, the Fermi level will move towards the conduction band edge, and the negative charge state occupancy of the Zn vacancy will increase. The trapping efficiency of positrons

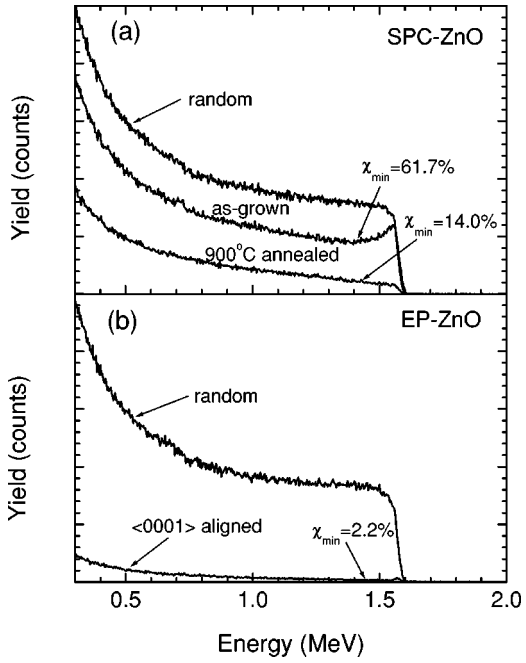

FIG. 3. RBS spectra in (a) as-grown and 900 °C annealed SPC–ZnO and (b) as-grown EP–ZnO.

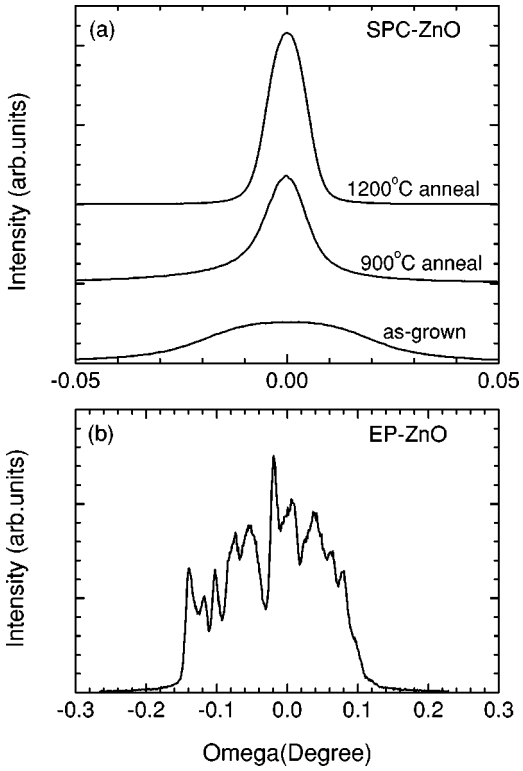

FIG. 4. XRD rocking curves measured for (a) SPC–ZnO annealed at different temperatures and (b) as-grown EP–ZnO.

would then increase, resulting in an increase in the average positron lifetime.

Figure 3(a) shows the RBS spectra obtained from the as-grown and 900 °C annealed SPC–ZnO. In the as-grown SPC–ZnO, the aligned backscattering spectrum is very high, which suggests poor crystal quality, and may be due to native defects. After 900 °C annealing where positron lifetime decreases in Fig. 2, the level of the aligned spectrum decreases drastically. The $\chi_{\min}$ before and after annealing is 61.7% and 14%, respectively. This shows that annealing can improve the crystal quality to a large extent, possibly due to the decrease of defects. The increase of crystal quality after annealing in ZnO was also observed by other authors.[28,35]

Figure 3(b) shows the RBS spectrum for the as-grown EP–ZnO. Contrary to the SPC–ZnO, the aligned spectrum exhibits fairly low yield, with $\chi_{\min}$ of only 2.2%, which means that the SPC–ZnO might contain much more defects than the EP–ZnO. Therefore, the RBS measurements confirm that the higher positron lifetime in SPC–ZnO than that of EP–ZnO might be due to its lower quality.

Figure 4(a) presents the (002) XRD rocking curves obtained from the as-grown and annealed SPC–ZnO crystals. The peak positions of these curves are shifted to 0° for the comparison of the result. In the as-grown SPC–ZnO, the FWHM is about 0.043°. After 900 °C annealing, the FWHM decreases drastically to 0.012°, and then it shows further decrease with increasing annealing temperature. The shape of the rocking curve also changes. After 900 °C annealing, the peak becomes much narrower, but there is still a small broad component in the tail. Further annealing eliminates the broad tail. These findings suggest that the crystal quality is improved after high temperature annealing. It coincides with the decrease of the defect concentration observed by PAS and RBS.

The XRD rocking curve for EP–ZnO is shown in Fig. 4(b). The rocking curve shows a very broad structure with many fine peaks. This suggests that the EP–ZnO includes mosaic structures. Similar mosaic structure of EP–ZnO had also been observed by Zeuner *et al.*[36] However, this mosaic structure is not observed by our RBS measurement, because the tilt angle of the columns with respect to each other is rather small (which can be reflected by the range of the x-ray rocking curve). That is, RBS is not sensitive to such a small tilt angle. The positron lifetime measurement is also not sensitive to this mosaic structure as long as each column is relatively large compared to the positron diffusion length ($\sim$100 nm). Inside each column, the EP–ZnO crystal contains less defects than the SPC–ZnO. Hence the RBS yield is much lower, and the positron lifetime is shorter in EP–ZnO. In other words, the EP–ZnO has lower crystallinity than the SPC–ZnO, but it has much better quality with regards to the impurities or defects.

B. Electrical and optical measurements

All the SPC–ZnO samples before and after annealing show *n*-type conductivity. The measured electron concentration n_e, resistivity ρ, and Hall mobility μ are listed in Table I. The electron concentration dramatically increases due to annealing. After 900 °C annealing, n_e increases by approximately two orders of magnitude from the as-grown state. Probably this can be connected with the disappearance of grown-in defects as seen in PAS, RBS, and XRD measurements. After 1200 °C annealing, n_e further increases. This may be connected with the evaporation of oxygen during

TABLE I. Free electron concentration n_e, resistivity ρ, and electron mobility μ in the as-grown and annealed SPC–ZnO determined from the Hall measurements.

T_a (°C)	ρ (Ω cm)	n_e (cm^{-3})	μ ($cm^2\ V^{-1}\ s^{-1}$)
As-grown	1.7×10^4	5.7×10^{12}	66
900	247	3.6×10^{14}	70
1200	0.88	1.4×10^{17}	51

annealing, because both the V_O and I_{Zn} are thought to be shallow donors.[31,37,38] After 1200 °C annealing, even though the increase of positron lifetime might indicate introduction of V_{Zn} acceptor states, they are overcompensated with these donors. That is, the introduction rate of V_{Zn} might be much lower than that of V_O and I_{Zn}. The Hall mobility does not show major changes below 1200 °C, i.e., 50–70 $cm^2\ V^{-1}\ s^{-1}$. This means the electron scattering centers still remain after annealing. Moreover, this mobility is still lower than that of EP–ZnO (about 200 $cm^2\ V^{-1}\ s^{-1}$).[2] This demonstrates different quality between SPC–ZnO and EP–ZnO.

Figure 5 shows the CL spectra of as-grown and annealed SPC–ZnO. The EP–ZnO sample was also measured for comparison. In the as-grown SPC–ZnO, only one peak with a small intensity appears at about 3.3 eV. This room temperature UV luminescence is due to the recombination through free excitons.[34,39–41] For the annealed SPC–ZnO samples, besides the UV emission, another peak also appears, which ranges from 2.1 to 2.3 eV. This is so-called green emission.

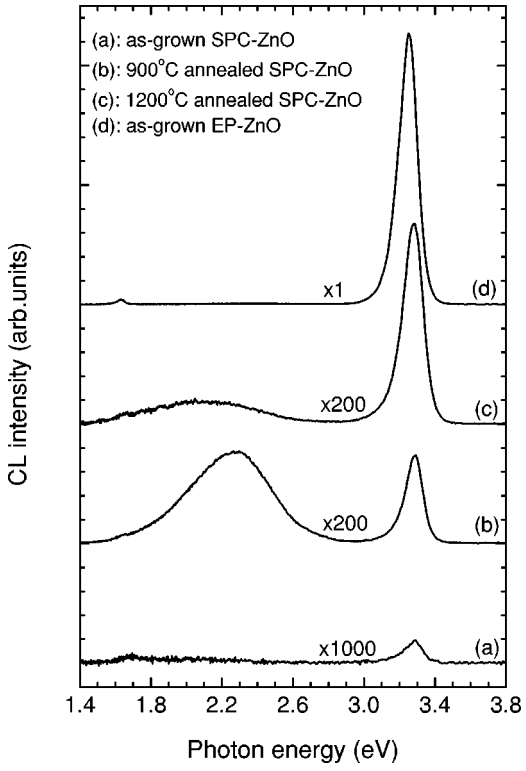

FIG. 5. Cathodoluminescence spectra obtained for the as-grown and annealed SPC–ZnO and as-grown EP–ZnO.

The origin of this optical transition is still under discussion, but it may be mediated by some deep level defects or impurities.[24,25,42–45]

We note that the UV emission is systematically enhanced after annealing. In the as-grown sample, there might be large number of deep level defects acting as nonradiative recombination centers to weaken the UV emission. The enhancement of UV emission after annealing reflects the improvement of the crystal quality. This shows good correlation with PAS, RBS, and XRD observation described earlier.

The green emission intensity also changes after annealing. At first it increases with annealing temperature, then it deceases at the highest temperature (1200 °C). The peak position also shifts slightly to lower energy. In the as-grown material, this emission is invisible. It may be due to the existence of some nonradiative recombination centers which compete with green emission, and these centers can be eliminated by annealing. Therefore green luminescence shows an increase at 900 °C. It should be pointed out that the increase of green emission may also originate for other reasons, such as the increase of the radiative deep centers, or the change of the defect occupancy. The latter case is more probable, as the Fermi level increases significantly after annealing due to an increase of the carrier concentration. The reason for the decrease of green emission after 1200 °C annealing is not fully understood. Possibly, it is due to the reappearance of some other deep level defects, which can be reflected by a change in the green emission peak position. Further detailed experiments about the effect of annealing on the green luminescence are under consideration.

In the as-grown EP–ZnO, the peak of the UV emission is more than three orders of magnitude higher than that of as-grown SPC–ZnO. This again confirms that the EP–ZnO contains much less nonradiative recombination centers.

IV. CONCLUSION

Positron annihilation spectroscopy is used to study vacancy defects in ZnO single crystals. In hydrothermal grown ZnO, V_{Zn}-related defects were found to exist. Annealing experiments show that V_{Zn}-related defects disappear at about 600 °C. Further annealing above 1000 °C produces V_{Zn}-related defects again. RBS and XRD measurements show the improvement of the crystal quality after annealing. This might be due to the reduction of point defects and rearrangement of crystal grains. The electron concentration increases after high temperature annealing. This is explained as the disappearance of acceptor states probably due to V_{Zn}-related defects and the evaporation of oxygen and the subsequent introduction of either oxygen vacancies or Zn interstitials. The UV light emission is enhanced with increasing annealing temperature, suggesting the disappearance of nonradiative recombination centers by heating. The ZnO crystal quality is affected by both simple point defects and extended defects.

ACKNOWLEDGMENTS

The authors thank Professor M. J. Puska for providing them with the computer code to calculate positron lifetime.

They also thank Dr. T. Oshima and Dr. A. Ohi for their kind help in the Hall measurements. This work was partly supported by the Nuclear Energy Generic Crossover Research Project promoted by Ministry of Education, Culture, Sports, Science and Technology of Japan.

[1] F. C. M. Van de Pol, Ceram. Bull. **69**, 1959 (1990).
[2] D. C. Look, D. C. Reynolds, J. R. Sizelove, R. L. Jones, C. W. Litton, G. Cantwell, and W. C. Harsch, Solid State Commun. **105**, 399 (1998).
[3] Y. Chen, D. Bagnall, and T. Yao, Mater. Sci. Eng., B **75**, 190 (2000).
[4] D. C. Look, Mater. Sci. Eng., B **80**, 383 (2001).
[5] D. C. Look, D. C. Reynolds, J. W. Hemsky, R. L. Jones, and J. R. Sizelove, Appl. Phys. Lett. **75**, 811 (1999).
[6] S. B. Zhang, S.-H. Wei, and A. Zunger, J. Appl. Phys. **83**, 3192 (1998).
[7] R. Krause-Rehberg and H. S. Leipner, *Positron Annihilation in Semiconductors, Defect Studies*, Springer Series in Solid-State Sciences **127** (Springer, Berlin, 1999), Vol. 127.
[8] T. K. Gupta, W. D. Straub, M. S. Ramanachalam, J. P. Schaffer, and A. Rohatgi, J. Appl. Phys. **66**, 6132 (1989).
[9] M. S. Ramanachalam, A. Rohatgi, J. P. Schaffer, and T. K. Gupta, J. Appl. Phys. **69**, 8380 (1991).
[10] J. Zhong, A. H. Kitai, P. Mascher, and W. Puff, J. Electrochem. Soc. **140**, 3644 (1993).
[11] W. Puff, S. Brunner, and P. Mascher, in *22nd International Conference on the Physics of Semiconductors*, edited by D. J. Lockwood (World Scientific, Singapore, 1995) Vol. 3, p 2439.
[12] R. M. de la Cruz, R. Pareja, R. González, L. A. Boatler, and Y. Chen, Phys. Rev. B **45**, 6581 (1992).
[13] S. Brunner, W. Puff, A. G. Balogh, and P. Mascher, Mater. Sci. Forum **363–365**, 141 (2001).
[14] A. Uedono, T. Koida, A. Tsukazaki, M. Kawasaki, Z. Q. Chen, S. F. Chichibu, and H. Koinuma, J. Appl. Phys. **93**, 2481 (2003).
[15] P. Kirkegaard, N. J. Pederson, and M. Eldrup, Risø National Laboratory, DK-4000 Roskilde, Denmark, 1989.
[16] Y. Ohta, T. Haga, and Y. Abe, Jpn. J. Appl. Phys., Part 2 **36**, L1040 (1997).
[17] C. Boemare, T. Monteiro, M. J. Soares, J. G. Guilherme, and E. Alves, Physica B **308–310**, 985 (2001).
[18] L. J. Van der Pauw, Philips Res. Rep. **13**, 1 (1958).
[19] T. Sekiguchi and K. Sumino, Rev. Sci. Instrum. **66**, 4277 (1995).
[20] R. B. Gregory and Y. Zhu, Nucl. Instrum. Methods Phys. Res. A **290**, 172 (1990).
[21] A. F. Kohan, G. Ceder, D. Morgan, and Chris G. Van de Walle, Phys. Rev. B **61**, 15019 (2000).
[22] E.-C. Lee, Y.-S. Kim, Y.-G. Jin, and K. J. Chang, Phys. Rev. B **64**, 085120 (2001).
[23] S. B. Zhang, S.-H. Wei, and A. Zunger, Phys. Rev. B **63**, 075205 (2001).
[24] P. H. Kasai, Phys. Rev. B **130**, 989 (1963).
[25] K. Vanheusden, C. H. Seager, W. L. Warren, D. R. Tallant, and J. A. Voigt, Appl. Phys. Lett. **68**, 403 (1996).
[26] M. J. Puska, S. Mäkinen, M. Manninen, and R. M. Nieminen, Phys. Rev. B **39**, 7666 (1989).
[27] M. J. Puska and R. M. Nieminen, J. Phys. F: Met. Phys. **13**, 333 (1983).
[28] K. Ogata, K. Sakurai, Sz. Fujita, Sg. Fujita, and K. Matsushige, J. Cryst. Growth **214–215**, 312 (2000).
[29] E. Ziegler, A. Heinrich, H. Oppermann, and G. Stöver, Phys. Status Solidi A **66**, 635 (1981).
[30] A. Hausmann and B. Utsch, Z. Phys. B **21**, 217 (1975).
[31] K. I. Hagemark, J. Solid State Chem. **16**, 293 (1976).
[32] T. Sekiguchi, S. Miyashita, K. Obara, T. Shishido, and N. Sakagami, J. Cryst. Growth **214**, 72 (2000).
[33] T. Sekiguchi, N. Ohashi, and Y. Terada, Jpn. J. Appl. Phys., Part 2 **36**, L289 (1997).
[34] T. Sekiguchi, N. Ohashi, and Y. Terada, Mater. Sci. Forum **258–263**, 1371 (1998).
[35] M. K. Puchert, P. Y. Timbrell, and R. N. Lamb, J. Vac. Sci. Technol. A **14**, 2220 (1996).
[36] A. Zeuner, H. Alves, D. M. Hofmann, B. K. Meyer, M. Heuken, J. Bläsing, and A. Krost, Appl. Phys. Lett. **80**, 2078 (2002).
[37] G. D. Mahan, J. Appl. Phys. **54**, 3825 (1983).
[38] D. C. Look, J. W. Hemsky, and J. R. Sizelove, Phys. Rev. Lett. **82**, 2552 (1999).
[39] P. Zu, Z. K. Tang, G. K. L. Wong, M. Kawasaki, A. Ohtomo, H. Koinuma, and Y. Segawa, Solid State Commun. **103**, 459 (1997).
[40] D. M. Bagnall, Y. F. Chen, M. Y. Shen, Z. Zhu, T. Goto, and T. Yao, J. Cryst. Growth **184/185**, 605 (1998).
[41] D. W. Hamby, D. A. Lucca, M. J. Klopfstein, and G. Cantwell, J. Appl. Phys. **93**, 3214 (2003).
[42] D. C. Reynolds, D. C. Look, B. Jogai, and H. Morkoç, Solid State Commun. **101**, 643 (1997).
[43] D. C. Reynolds, D. C. Look, B. Jogai, J. E. Van Nostrand, R. Jones, and J. Jenny, Solid State Commun. **106**, 701 (1998).
[44] B. Lin, Z. Fu, and Y. Jia, Appl. Phys. Lett. **79**, 943 (2001).
[45] N. Y. Garces, L. Wang, L. Bai, N. C. Giles, L. E. Halliburton, and G. Cantwell, Appl. Phys. Lett. **81**, 622 (2002).